Passive, Broadband, and Low-Frequency Suppression of Laser Amplitude Noise to the Shot-Noise Limit Using a Hollow-Core Fiber

Euan J. Allen,[1,2,*] Giacomo Ferranti,[1] Kristina R. Rusimova,[3] Robert J.A. Francis-Jones,[3,†] Maria Azini,[3] Dylan H. Mahler,[1,‡] Timothy C. Ralph,[4] Peter J. Mosley,[3] and Jonathan C.F. Matthews[1]

[1] *Quantum Engineering Technology Labs, H. H. Wills Physics Laboratory, and Department of Electrical and Electronic Engineering, University of Bristol, Bristol BS8 1FD, United Kingdom*

[2] *Quantum Engineering Centre for Doctoral Training, Nanoscience and Quantum Information Centre, University of Bristol, Bristol BS8 1FD, United Kingdom*

[3] *Centre for Photonics and Photonic Materials, Department of Physics, University of Bath, Bath BA2 7AY, United Kingdom*

[4] *Centre for Quantum Computation and Communication Technology, School of Mathematics and Physics, University of Queensland, Brisbane, Queensland 4072, Australia*

(Received 18 June 2019; published 31 October 2019)

Reducing noise to the shot-noise limit is a challenge for laser development for ultrasensitive applications in precision sensing and fundamental science. We use hollow-core fiber in a collinear-balanced-detection scheme to suppress 2.6 dB of amplitude noise to within 0.01 dB of the shot-noise limit, while simultaneously preserving the spectrum and temporal profile of picosecond laser pulses. We also provide an enhanced version of the scheme that concatenates multiple circuits for suppression over many frequencies and broad frequency ranges. We perform a first demonstration of this method and reduce total excess amplitude noise, between 2 and 6 MHz, by 85%. These demonstrations enable passive, broadband, all-guided fiber-laser technology operating at the shot-noise limit.

DOI: 10.1103/PhysRevApplied.12.044073

I. INTRODUCTION

Doped fiber lasers are attractive due to their low cost, compact size, and robust stable operation. However, they exhibit classical intensity noise well above the optical shot-noise limit due to stimulated spontaneous emission [1–4]. To suppress this extra noise, existing noise-suppression techniques could, in principle, enable use of fiber lasers for ultrasensitive applications. However, direct changes to the laser itself, such as intracavity spectral filtering [5] and optical feedback into the laser cavity [6,7], or external methods, such as feedback or feedforward circuits coupled to an optical modulator [8,9] or external cavity filtering [10], all require fast and low-noise electronics. The speed of such electronics limits the bandwidth that can be filtered, while electronic noise can be transferred back into the optical beam.

In practice, the ability of these schemes to reach the shot-noise limit can be hindered by fundamental limitations of two beams output from a beam splitter being uncorrelated on the quantum level [11]. They can also suffer from technical issues such as nonzero time response of any feedback mechanism [12], beam-geometry and pointing issues [9], and the trade-off when tailoring the speed or gain of the feedback mechanism to reduce noise across a large bandwidth [8–10,12]. Removal of common-mode noise using balanced detection [13] is passive; however, optical intensity must be equally split across the two detectors to remove all classical noise, and this is impossible for optical transmission measurements or imaging whenever the sample introduces unknown loss before detection.

II. COLLINEAR BALANCED DETECTION

Collinear balanced detection (CBD) is a passive method that requires no knowledge of beam intensity and no intensity subtraction [14]. It comprises an optical delay in a static asymmetric Mach-Zehnder interferometer (AMZI) to provide an output beam with shot-noise-limited intensity fluctuation at one frequency. This was used, with a free-space delay of 8.6 m, to increase the quality of stimulated Raman microscopy measured at 17.5 MHz [14] and to suppress classical noise from a noisy fiber laser used to generate amplitude-squeezed light with intensity fluctuations below the optical shot-noise limit at 20–24

*euan.allen@bristol.ac.uk

†Present address: Clarendon Laboratory, University of Oxford, Parks Road, Oxford OX1 3PU, United Kingdom.

‡Present address: Xanadu, 372 Richmond Street West, Toronto, Ontario M5V 2L7, Canada.

MHz [15]. However, two criticisms of CBD are that existing demonstrations have used free-space delays, which require the stability of optical isolation tables, and that existing CBD demonstrations suppress noise at only one frequency [16]. Here we address both points by demonstrating a fiber-optic approach that is more robust than a free-space approach and we introduce an iterated approach that allows suppression of noise at multiple frequencies simultaneously.

The original CBD concept is illustrated in Fig. 1(a). A train of laser pulses are launched into one input of an AMZI, where one path inside imparts a relative time delay of $\tau = Ln/c$ (L is the length of delay medium of refractive index n) such that the pulses in the delayed and nondelayed paths do not overlap in time when their paths recombine at the second beam splitter. Because the pulses do not optically interfere at the second beam splitter, the AMZI requires no phase stabilization. Output from the CBD circuit, for a given τ, are two beams that both have a classical-noise-suppression factor Υ, which follow a sinusoidal function [Fig. 1(b)] that reaches the shot-noise limit at odd multiples of $f = 1/2\tau$ [14],

$$\Upsilon(f) = \frac{1}{2}(1 + \cos \pi f \tau), \tag{1}$$

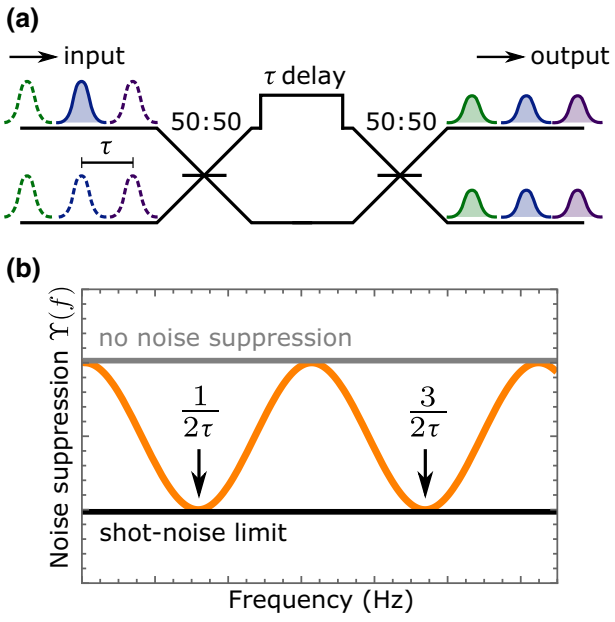

FIG. 1. (a) Collinear-balanced-detection setup that produces shot-noise-limited light at the output of the interferometer with double the repetition rate, half the average power, and a quarter of the peak power of the original pulse train. (b) Theoretical plot [Eq. (1)] of classical noise suppressed by CBD over a range of noise frequencies given a single delay of τ. CBD causes complete suppression of odd multiples of the frequency $f = 1/2\tau$ at both outputs.

where $\Upsilon(f) = 1$ or $\Upsilon(f) = 0$ indicates that either zero or total classical noise suppression has occurred, respectively (the latter becoming shot noise limited). To remove noise at a frequency f, a delay of length $L = c/2nf$ should be implemented.

The inverse relation with the suppression frequency ($\tau = 1/2f$) means the delay required for suppression of lower-frequency noise becomes increasingly challenging to build and maintain in free space. For example, suppressing noise at 5 MHz requires 30 m of free-space delay. Constructing a waveguided delay long enough to suppress noise at low frequencies therefore makes CBD more practical and would allow integration of passive all-guided noise suppression with fiber lasers. Solid-core optical fiber, such as SMF-28 fiber, has the potential to filter noise at subkilohertz frequencies because of the availability of lengths of many kilometers—we illustrate this in Supplemental Material [32] with results for a 4.3-km delay that suppresses amplitude noise at 25 kHz. However, self-phase modulation and dispersion occur when laser pulses traverse solid-core fiber, which for the CBD scheme results in half of the output pulses being spectrally broadened and temporally elongated; this is undesirable when the filtered light is to be used for applications sensitive to the spectral and temporal profile of laser pulses, such as nonlinear spectroscopy and nonlinear microscopy, or inducing nonlinear processes, such as to generate nonclassical states of light. Furthermore, Raman scattering in solid-core fiber will cause extra noise in the output optical beam of the CBD circuit [17], which will negate the noise-suppression goal.

III. RESULTS

A. Implementation in hollow-core fiber

To avoid the nonlinear effects of conventional fiber, we use hollow-core fiber (HCF) that guides light predominantly in an air-filled core. Here we use recently developed free-boundary (or antiresonant) HCF that has a simple cladding structure comprising a single ring of silica capillaries fused to a fiber jacket (inset in Fig. 2). The fiber guides light along the core via resonant trapping through the capillary structures [18]. Hence, low-loss guidance along the fiber can be achieved across broad wavelength ranges [19,20]. The fundamental mode propagates in a large core with almost no overlap with the glass to minimize nonlinearity and dispersion (see Fig. 2), while careful control of the capillary dimensions during fabrication enables higher-order modes to be suppressed yet bend loss in the fundamental mode to remain manageable [21]. This simple structure enables fabrication of hundreds of meters of fiber with consistent properties and a high damage threshold [22].

Hollow-core fiber is fabricated by the stack-and-draw process, forming a fiber of six capillaries with an average

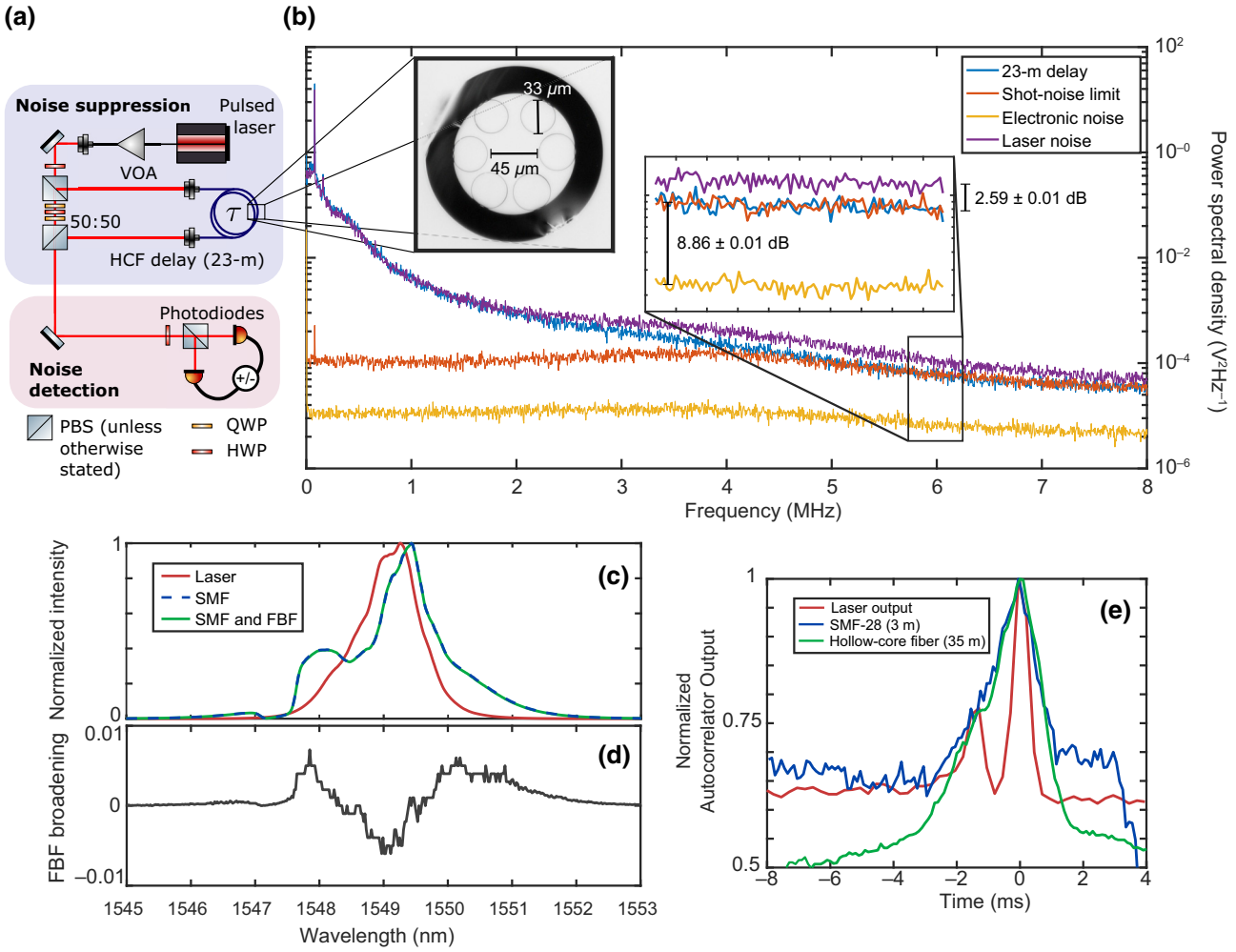

FIG. 2. (a) The optical setup used to construct the asymmetric Mach-Zender interferometer used for noise suppression and the balanced-detection technique to measure optical noise. The inset shows the structure of the free-boundary fiber (FBF). (b) Measurement results, removing all classical noise at the expected frequency of approximately 6.5 MHz reaching within 0.011 ± 0.008 dB of the shot-noise limit (averaging the signal in a 0.5-MHz bandwidth centered at 6.5 MHz). Displayed are the noise in the laser without filtering (purple) and with filtering (blue), the equivalent power shot-noise limit (red), and electronic noise floor (yellow). The optical nose data here are included in Fig. 4(b), plotted as a noise-suppression ratio [Eq. (1)]. The common-mode rejection ratio for detection in this experiment is greater than 34 dB, and all measurements are performed with a total power of 330 μW incident on the balanced detector. (c) The additional spectral broadening induced by the introduction of 35 m of FBF into the experiment compared with that induced by less than 1 m of SMF-28 fiber. (d) The percentage change in the spectrum induced by the FBF, demonstrating that it causes a change of less than 1% compared with when it is not present. (e) Comparison of the temporal dispersion introduced by a length of hollow-core free-boundary fiber. The dispersion is comparable with the dispersion introduced by 3 m of SMF-28 fiber. HWP half-waveplate; PBS, polarizing beam splitter; QWP, quarter-waveplate; SMF, single-mode fiber; VOA, variable optical attenuator.

diameter of 33 μm surrounding a 45-μm core. The fiber has an outer diameter of 160 μm and the thickness of the capillary walls are estimated to be 520 nm. The attenuation of the fundamental mode in the fiber at a wavelength of 1550 nm is found by a cutback measurement on 34 m of fiber to be approximately 0.07 dB/m. By comparison with lengths of conventional single-mode fiber (SMF-28), dispersion of the HCF is estimated to be 1.5 ps/nm per kilometer, which is 9% of that for conventional single-mode fiber [see Fig. 2(e)]. To minimize bend loss within the HCF, the fiber is laid out on a piece of card in a circle of approximately 60-cm diameter.

The nonlinearity of the HCF is estimated by our measuring of self-phase-modulation-induced nonlinear spectral broadening of the pulses after propagation along a 35-m-HCF delay using an Anritsu MS9740A optical spectrum analyzer. The source of pulsed light is a Pritel FFL laser that emits 2-ps pulses at 1550 nm with peak powers of approximately 200 W. For coupling into the HCF, the pulses propagate through a short length (less than 1 m)

of SMF-28 fiber. Because of this, comparisons are made between propagation through both the SMF-28 fiber and the HCF, and then bypassing the HCF and only propagation along the SMF-28 fiber. Figure 2(c) demonstrates that for pulses of this power, the HCF adds negligible amounts of spectral broadening, substantially less than the short amount of solid-core single-mode fiber. Figure 2(d) demonstrates a change of less than 1% in the broadening caused by the free-boundary fiber for any particular wavelength component.

The HCF dispersion is investigated with a Toptica FemtoFErb 1560 laser. This laser emits pulses with a 58-fs temporal profile that are approximately 70 nm wide in the optical spectrum. The effects of dispersion caused by the HCF are shown in Fig. 2(e). When compared with conventional SMF-28 fiber, the dispersion in 35 m of hollow-core fiber is comparable with the dispersion in 3 m of SMF-28 fiber (which has a quoted dispersion of 18 ps/nm per kilometer [23]). As such we can predict that the dispersion in the HCF is approximately an order of magnitude less than that expected from refractive-index-contrast fibers (1.5 ps/nm per kilometer).

We first construct the CBD circuit in Fig. 2(a) with a 23-m-HCF delay. A half-waveplate and a polarizing beam splitter replace each balanced beam splitter to fine-tune the splitting ratio to compensate for any unbalanced loss in the delay path. Detection of the amplitude noise and the shot noise of the laser light is performed by self-homodyne detection [17,24], where the incident light is split by a balanced beam splitter and detected by two identical photodiodes (Thorlabs FGA01FC with custom amplification circuits). The signals from each photodiode are first filtered via dc (Mini-Circuits BLK-89-S+) and low-pass (Mini-Circuits BLP-21.4+) electronic filters and are then sent to individual channels of a Keysight InfiniiVision MSOX3104A oscilloscope (operated at 2.5 gigasamples/s). The low-pass filters remove high-frequency noise from the detectors, allowing a higher-resolution measurement of the optical noise at the frequencies of interest. The dc filter allows comparisons of noise at different incident powers to be made without concern for the offset change on the oscilloscope signal. All data captures are taken with a time resolution of 20 μs and with maximum voltage resolution possible for the amplitude of the signal (typically 5–10 mV per division). The signals are logged on a desktop personal computer, digitally added to or subtracted from one another, and then Fourier transformed to the frequency domain to allow comparison of particular Fourier components of the noise. Subtraction of the photocurrents provides a shot-noise reference for the incident power, and addition of the photocurrents provides the noise present in the incoming laser light.

Light from the laser is first attenuated by a digital variable optical attenuator (Oz Optics DA-100) to attenuate the optical power to work within the range of the detection system, before being launched into free space. The light is split into each path of the AMZI by a half-waveplate and polarizing beam splitter. Waveplates in the nondelayed path match the polarization of the two paths. The pulse trains are recombined on a second (nonpolarizing) beam splitter and the noise characteristics are measured. The output of the SMF-28 fiber from the pulsed fiber laser is coupled into free space via a three-axis stage system (Elliot Scientific) with an aspheric lens system (f = 3.1 mm, Thorlabs C330TMD-C). Coupling into the HCF uses an identical system but with a f = 11.0 mm (Thorlabs C220TMD-C) lens to allow for mode matching into the large core.

The laser used is an erbium-doped silica fiber laser that is passively mode locked with a fiber-coupled output and generates 2-ps pulses centered at a wavelength of 1550 nm with a repetition rate of 50 MHz (Pritel FFL). Without operation of the CBD circuit, our laser exhibits super-Poissonian amplitude noise present at all frequencies within the detector bandwidth (0–10 MHz). This is shown in Fig. 2(b)—the raw laser light (purple) contains noise contributions that are larger than the shot-noise limit (red). The laser's raw noise is measured by our blocking one of the paths of the interferometer and then reducing the attenuation of the variable optical attenuator to keep the power incident on the detectors the same in the suppressed and nonsuppressed configurations. The total loss in the delay path is 3.6 ± 0.2 dB, of which approximately 1 dB is from coupling in and out of the HCF and 1.6 dB is from propagation loss. With the HCF-CBD circuit in operation, amplitude noise is suppressed as shown in Fig. 2(b) (blue), reaching within 0.011 ± 0.008 dB of the shot-noise limit at 6.5 MHz, as predicted for the length of fiber used.

B. Large bandwidth suppression

Next we address the weakness that the original CBD scheme filters only at odd multiples of $f = 1/2\tau$ [16]. We use the stability of fiber delay to concatenate CBD circuits in series. As any individual CBD circuit does not add noise at any particular frequency, we find that by concatenating two CBD circuits, each with delays τ_1 and τ_2, noise suppression follows

$$\Upsilon(f) = \frac{1}{4}(1 + \cos \pi f \tau_1)(1 + \cos \pi f \tau_2). \qquad (2)$$

The theoretical noise suppression across a fixed band of frequencies is shown in Fig. 3.

The average noise reduction across any period of frequencies for a single delay is $\langle \Upsilon(f) \rangle_1 = \frac{1}{2}$, since integrating $0.5(1 + \cos x)$ [Eq. (1)] over a period of the function gives the value of a half. To investigate what the average noise reduction is for a double-delay scheme, we consider the subset of cases where $\tau_2 = k\tau_1$, with k taking only integer values. This simplifies the analysis since the function

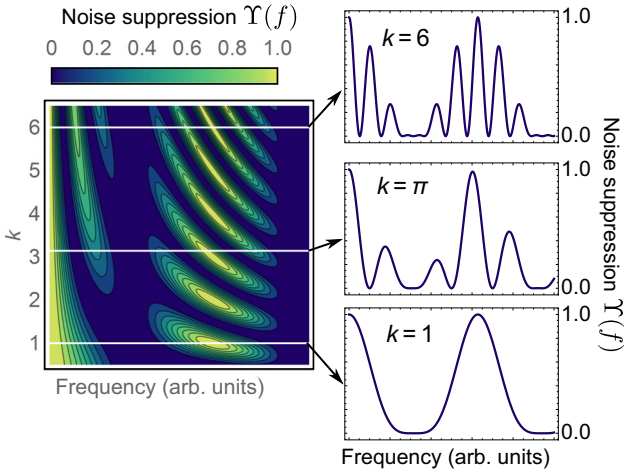

FIG. 3. Theoretical prediction for the double-CBD scheme. All plots show the amount of classical noise suppression from two noise-suppressing interferometers with delays τ_1 and $\tau_2 = k\tau_1$, respectively. Shown is a contour plot of the predicted noise suppression for arbitrary k, with inset examples for fixed $k = 6$, π, and 1.

$0.25(1+\cos x)(1+\cos kx)$ [Eq. (2)], for integer k, always has a period between 0 and 2π that we can integrate over to calculate the average noise reduction. The average noise reduction for two delays $\langle \Upsilon(f) \rangle_2$ is given by

$$\langle \Upsilon(f) \rangle_2 = \frac{1}{2\pi} \int_0^{2\pi} \frac{1}{4}(1+\cos x)(1+\cos kx)\, dx$$
$$= \frac{1}{8\pi} \left(\frac{2k^2-1}{(k^2-1)k} \sin 2\pi k + 2\pi \right).$$

For integer k only, $\sin 2\pi k = 0$ for all k, and so the average noise suppression simplifies to $\langle \Upsilon(f) \rangle_2 = 0.25$ for $k \geq 2$. For $k = 1$ a number of terms simultaneously tend to zero and so we find that

$$\lim_{k \to 1} \frac{2k^2-1}{(k^2-1)k} \sin 2\pi k = \pi, \tag{3}$$

and thus for $k = 1$, $\langle \Upsilon(f) \rangle_2 = 3/8 = 0.375$. Therefore, we find that for all integer values of k the average noise reduction takes the value of 0.25 apart from the unique value at $k = 1$ (interferometers with delays of the same length), where the average noise reduction is reduced to 0.375 of the original value. Noninteger values of k result in an integral range not covering an entire period of the functions in frequency space. Numerical analysis, where the integral range is tuned to always cover an entire period

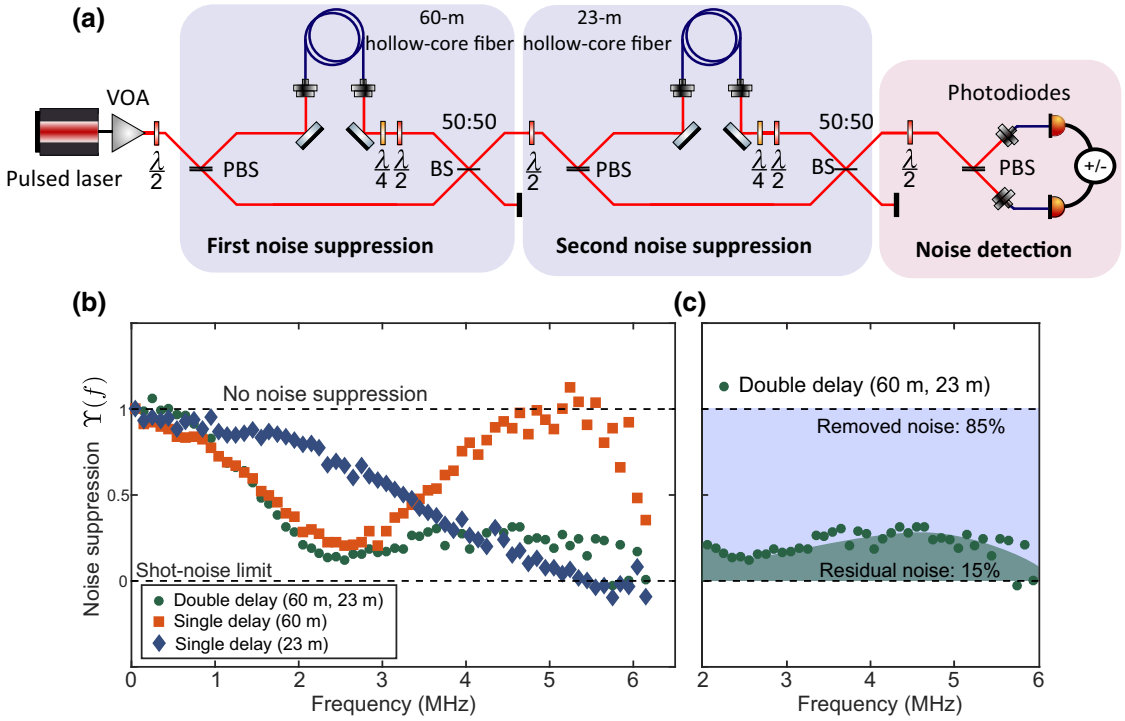

FIG. 4. (a) Experimental setup of two sequential CBD circuits. Each interferometer is constructed as per Fig. 2, but with now two lengths of 60 and 23 m used as the delays. (b) Experimental results for the performance of the double-CBD circuit, for a single delay of 23 m (blue), a single delay of 60 m (orange), and both delays (green) in operation in the setup. The 60-m single delay suppresses noise at a frequency that is almost 1 order of magnitude lower than previous demonstrations [14,15]. The 23-m-single-delay data are replotted from Fig. 2(b). (c) Repeated plot of experimental results for the double-CDB circuit from (b), plotted between 2 and 6 MHz, illustrating the 85% total noise reduction achieved across this bandwidth. BS, beam splitter; PBS, polarizing beam splitter; VOA, variable optical attenuator.

of the function for any rational value of k, indicates that the average noise reduction across a period is always 0.25 apart from the unique value at $k = 1$. Values of k that are irrational produce aperiodic functions.

To explore this for instances of τ_1 and τ_2, we build the setup shown in Fig. 4(a). Figure 4(b) displays the experimentally measured values of $\Upsilon(f)$, obtained with a half-waveplate and polarizing beam splitter as tunable beam splitters to switch between only one of each CBD circuit suppressing noise and both circuits suppressing noise simultaneously. The total noise suppression across the 2–6-MHz bandwidth for the double-CBD scheme is 85% of the original laser noise, which is shown in Fig. 4(c). For an equivalent bandwidth, the 23- and 60-m single-CBD implementations each remove less noise as expected: 55% and 41%, respectively.

IV. CONCLUSION

These demonstrations show free-boundary HCF can be used to implement CBD to suppress amplitude noise from a fiber laser at megahertz frequencies. The cost of each CBD circuit is loss of half of the average power and three quarters of the peak power—the same as passive temporal multiplexing used to increase laser repetition rate [25]. This suggests use where an overhead in power exists and the need for low-amplitude noise takes priority; for example, in ultrasensitive imaging [16,26–28] and squeezing experiments [29]. While solid-core fiber introduces the practicality of a waveguided optical delay, the detrimental nonlinear effects that it has on laser pulses prohibit its use in CBD. Instead, the low optical nonlinearity of air-guiding safeguards spectral and temporal properties of output laser pulses, while providing the practicality and stability of a waveguide to further enable concatenation of sequential CBD circuits to suppress amplitude noise at multiple frequencies. Further improvement of the HCF will allow a longer delay to be used for suppression at submegahertz frequencies: iterative design of the fiber structure could reduce propagation loss and lower nonlinearity and dispersion, or create anomalous regimes where soliton formation is possible [30]. An efficient interface between solid-core fiber and HCF will be needed for fully integrated noise suppression, and this has been shown to be possible with as little as 0.3-dB splice loss [31]. Generalization of CBD itself to continuous-wave light and temporal overlap of the pulses within the interferometer will further widen application, and will be the subject of future study.

Data are available at the University of Bristol data repository [33].

ACKNOWLEDGMENTS

We are grateful to Yu Shiozawa for assistance with detector electronics. This work was supported by EPSRC program Grant No. EP/L024020/1, the EPSRC UK Quantum Technology Hub in Quantum Enhanced Imaging (Grant No. EP/M01326X/1), U.S. Army Research Office Grant No. W911NF-14-1-0133, the EPSRC UK Quantum Technology Hub in Networked Quantum Information Technologies (Grant No. EP/M013243/1), the Innovate UK project FEMTO-AAD (Grant No. 102671), the Australian Research Council under the Centre of Excellence for Quantum Computation and Communication Technology (Grant No. CE170100012), and the Centre for Nanoscience and Quantum Information. E.J.A. was supported by the Bristol Quantum Engineering Centre for Doctoral Training, EPSRC Grant No. EP/L015730/1. J.C.F.M. acknowledges support from an EPSRC Early Careers Fellowship (Grant No. EP/M024385/1) and an ERC starting grant (Grant No. ERC-2018-STG 803665).

[1] Ibrahim Levent Budunoğlu, Coşkun Ülgüdür, Bulent Oktem, and Fatih Ömer Ilday, Intensity noise of mode-locked fiber lasers, Opt. Lett. **34**, 2516 (2009).

[2] Nathan R. Newbury and William C. Swann, Low-noise fiber-laser frequency combs (invited), J. Opt. Soc. Am. B **24**, 1756 (2007).

[3] R. Paschotta, Noise of mode-locked lasers (part I): Numerical model, Appl. Phys. B **79**, 153 (2004).

[4] WenJun Yue, YunXiang Wang, Cai-Dong Xiong, Zhi-Yong Wang, and Qi Qiu, Intensity noise of erbium-doped fiber laser based on full quantum theory, J. Opt. Soc. Am. B **30**, 275 (2013).

[5] Steve Sanders, Namkyoo Park, Jay W. Dawson, and Kerry J. Vahala, Reduction of the intensity noise from an erbium-doped fiber laser to the standard quantum limit by intracavity spectral filtering, Appl. Phys. Lett. **61**, 1889 (1992).

[6] O. Solgaard and K. Y. Lau, Optical feedback stabilization of the intensity oscillations in ultrahigh-frequency passively modelocked monolithic quantum-well lasers, IEEE Photonics Technol. Lett. **5**, 1264 (1993).

[7] R. Lang and K. Kobayashi, External optical feedback effects on semiconductor injection laser properties, IEEE J. Quantum Electron. **16**, 347 (1980).

[8] J. Alnis, A. Matveev, N. Kolachevsky, Th. Udem, and T. W. Hänsch, Subhertz linewidth diode lasers by stabilization to vibrationally and thermally compensated ultralow-expansion glass fabry-pérot cavities, Phys. Rev. A **77**, 053809 (2008).

[9] N. A. Robertson, S. Hoggan, J. B. Mangan, and J. Hough, Intensity stabilisation of an argon laser using an electro-optic modulator – performance and limitations, Appl. Phys. B **39**, 149 (1986).

[10] M. W. Hamilton, An introduction to stabilized lasers, Contemp. Phys. **30**, 21 (1989).

[11] Hans-Albert Bachor and Timothy C. Ralph, *A Guide to Experiments in Quantum Optics* (Wiley, Weinheim, Germany, 2004).

[12] Matthew S. Taubman, Howard Wiseman, David E. McClelland, and Hans-A. Bachor, Intensity feedback effects on quantum-limited noise, J. Opt. Soc. Am. B **12**, 1792 (1995).

[13] David M. Sonnenfroh, W. Terry Rawlins, Mark G. Allen, Claire Gmachl, Federico Capasso, Albert L. Hutchinson, Deborah L. Sivco, James N. Baillargeon, and Alfred Y. Cho, Application of balanced detection to absorption measurements of trace gases with room-temperature, quasi-cw quantum-cascade lasers, Appl. Opt. **40**, 812 (2001).

[14] Keisuke Nose, Yasuyuki Ozeki, Tatsuya Kishi, Kazuhiko Sumimura, Norihiko Nishizawa, Kiichi Fukui, Yasuo Kanematsu, and Kazuyoshi Itoh, Sensitivity enhancement of fiber-laser-based stimulated raman scattering microscopy by collinear balanced detection technique, Opt. Express **20**, 13958 (2012).

[15] Shota Sawai, Hikaru Kawauchi, Kenichi Hirosawa, and Fumihiko Kannari, Photon-number squeezing with a noisy femtosecond fiber laser amplifier source using a collinear balanced detection technique, Opt. Express **21**, 25099 (2013).

[16] Christian W. Freudiger, Wenlong Yang, Gary R. Holtom, Nasser Peyghambarian, Sunney X. Xie, and Khanh Q. Kieu, Stimulated raman scattering microscopy with a robust fibre laser source, Nat. Photonics **8**, 153 (2014).

[17] S. Schmitt *et al.*, Photon-number Squeezed Solitons from an Asymmetric Fiber-optic Sagnac Interferometer, Phys. Rev. Lett. **81**, 2446 (1998).

[18] N. M. Litchinitser, A. K. Abeeluck, C. Headley, and B. J. Eggleton, Antiresonant reflecting photonic crystal optical waveguides, Opt. Lett. **27**, 1592 (2002).

[19] David Bird, Attenuation of model hollow-core, anti-resonant fibres, Opt. Express **25**, 23215 (2017).

[20] Fei Yu, William J. Wadsworth, and Jonathan C. Knight, Low loss silica hollow core fibers for 3_4 μm spectral region, Opt. Express **20**, 11153 (2012).

[21] Walter Belardi and Jonathan C. Knight, Hollow antiresonant fibers with low bending loss, Opt. Express **22**, 10091 (2014).

[22] Piotr Jaworski, Fei Yu, Robert R. J. Maier, William J. Wadsworth, Jonathan C. Knight, Jonathan D. Shephard, and Duncan P. Hand, Picosecond and nanosecond pulse delivery through a hollow-core negative curvature fiber for micro-machining applications, Opt. Express **21**, 22742 (2013).

[23] Thorlabs, https://www.thorlabs.de/navigation.cfm, accessed: 2018-05-23.

[24] Ulrich Busk Hoffn, Integrated Quantum Optics: Experiments towards integrate quantum-light sources and quantum-enhanced sensing, Ph.D. thesis, Department of Physics, Technical University of Denmark (2007).

[25] M. A. Broome, M. P. Almeida, A. Fedrizzi, and A. G. White, Reducing multi-photon rates in pulsed down-conversion by temporal multiplexing, Opt. Express **19**, 22698 (2011).

[26] Michael A. Taylor and Warwick P. Bowen, Quantum metrology and its application in biology, Phys. Rep. **615**, 1 (2016).

[27] Alessio Gambetta, Vikas Kumar, Giulia Grancini, Dario Polli, Roberta Ramponi, Giulio Cerullo, and Marco Marangoni, Fiber-format stimulated-raman-scattering microscopy from a single laser oscillator, Opt. Lett. **35**, 226 (2010).

[28] Jaime Ortega Arroyo and Philipp Kukura, Non-fluorescent schemes for single-molecule detection, imaging and spectroscopy, Nat. Photonics **10**, 11 (2016).

[29] U. L. Andersen, T. Gerhing, C. Marquardt, and G. Leuchs, 30 years of squeezed light generation, Phys. Scr. **91**, 053001 (2016).

[30] Jonathan C. Knight, Photonic crystal fibres, Nature **424**, 847 (2003).

[31] R. Thapa, K. Knabe, K. L. Corwin, and B. R. Washburn, Arc fusion splicing of hollow-core photonic bandgap fibers for gas-filled fiber cells, Opt. Express **14**, 9576 (2006).

[32] See Supplemental Material at http://link.aps.org/supplemental/10.1103/PhysRevApplied.12.044073 for implementation of a collinear balanced detection scheme using a 4.3 km solid core fiber delay.

[33] E. J. Allen, G. Ferranti, K. R. Rusimova, R. J. A. Francis-Jones, M. Azini, D. H. Mahler, T. C. Ralph, P. J. Mosley, and Jonathan C. F. Matthews, Data for: "Passive, broadband, and low-frequency suppression of laser amplitude noise to the shot-noise limit using a hollow-core fiber," University of Bristol, https://doi.org/10.5523/bris.3u9log9k6begn27y0korx813xn (2019).